AMERICAN MUSEUM NOVITATES

Number 3881, 26 pp. June 19, 2017

A New Species of Nectar-feeding Bat of the Genus *Hsunycteris* (Phyllostomidae: Lonchophyllinae) from Northeastern Peru

PAÚL M. VELAZCO,[1] J. ANGEL SOTO-CENTENO,[1] DAVID W. FLECK,[2] ROBERT S. VOSS, [1] AND NANCY B. SIMMONS[1]

ABSTRACT

A new species of the nectarivorous bat genus *Hsunycteris* is described from lowland Amazonian forest in northeastern Peru. The new species, *H. dashe*, can be distinguished from other congeners by its larger size; V-shaped array of dermal chin papillae separated by a wide basal cleft; metacarpal V longer than metacarpal IV; broad rostrum; lateral margin of infraorbital foramen not projecting beyond rostral outline in dorsal view; well-developed sphenoidal crest; large outer upper incisors; weakly developed lingual cusp on P5; and well-developed, labially oriented M1 parastyle. A phylogenetic analysis of cytochrome-*b* sequence data indicates that *H. dashe* is sister to a clade that includes all other species of the genus including *H. cadenai*, *H pattoni*, and a paraphyletic *H. thomasi*. We provide a key based on craniodental and external characters of all four known species of *Hsunycteris*.

INTRODUCTION

The Neotropical bat genus *Hsunycteris* includes three described species of nectarivorous bats belonging to the phyllostomid subfamily Lonchophyllinae (Parlos et al., 2014). The combined geographic ranges of these species extend from Panama to central Bolivia (Woodman and Timm, 2006). *Hsunycteris* species can be distinguished from other lonchophyllines by a combination of the following characteristics: small size (GLS 19.5–22.5 mm,

[1] Division of Vertebrate Zoology (Mammalogy), American Museum of Natural History.
[2] Division of Anthropology, American Museum of Natural History.

 ISSN 0003-0082

FA 30.0–34.0 mm), bases of dorsal pelage hairs paler than tips, uropatagium not conspicuously furred, rostrum shorter than braincase, infraorbital foramen above anterior root of the second upper premolar, first and second upper premolars elongated, and central cuspid of lower premolars not deflected labially (Parlos et al., 2014; Cirranello et al., 2016). Prior to the revision of Parlos et al. (2014), species of *Hsunycteris* were included in the genus *Lonchophylla*, but the latter taxon was found to be paraphyletic with respect to other lonchophylline genera in numerous studies (Dávalos and Jansa, 2004; Woodman and Timm, 2006; Woodman, 2007; Dávalos et al., 2012; Dávalos et al., 2014). Parlos et al. (2014) described *Hsunycteris* to include three species of a previously unnamed clade that is the sister group of a larger clade comprising all other lonchophyllines (*Lonchophylla* sensu stricto, *Lionycteris*, *Xeronycteris*, and *Platalina*).

As currently recognized, *Hsunycteris* comprises three species: *H. cadenai*, *H. pattoni*, and *H. thomasi*. Allen (1904) described *Lonchophylla thomasi* (= *Hsunycteris thomasi*) based on one male specimen collected in the state of Bolívar, Venezuela. *Hsunycteris thomasi* is the most widespread species, with a distribution that almost matches that of the genus. Neither Woodman and Timm (2006) nor Griffiths and Gardner (2008) recognized subspecies of *H. thomasi*, but several studies agree that it is most likely a paraphyletic species complex (Clare et al., 2011; Parlos et al., 2014). Parlos et al. (2014) analyzed mitochondrial and nuclear genes and identified two lineages in *H. thomasi*, one of which is apparently more closely related to *H. pattoni* than to the other putative lineage of *H. thomasi*. Since both lineages of *H. thomasi* include specimens collected close to the type locality for this species and no known morphological traits can be used to distinguished these lineages, it is difficult to determine which individuals correspond to *H. thomasi* sensu stricto and which represent an unnamed species.

Woodman and Timm (2006) described the other two species of the genus. *Hsunycteris cadenai* is known from three localities in western Colombia (Woodman and Timm, 2006; Mantilla-Meluk et al., 2010). *Hsunycteris pattoni* was originally described from a single specimen from southeastern Peru, but is now known from five additional localities in Colombia, Ecuador, Peru, and Bolivia (Woodman and Timm, 2006; Mantilla-Meluk et al., 2009; Mantilla-Meluk et al., 2010; Parlos et al., 2014). No subspecies are recognized in either species (Parlos et al., 2014).

Recent faunal inventory work in the Yavarí-Ucayali interfluvial region of the Peruvian Amazon has resulted in the collection of three specimens of *Hsunycteris* that do not fit the diagnosis of any previously described species in the genus. We analyzed morphological, morphometric, and molecular data to describe these specimens as representing a new species of *Hsunycteris* and place this new taxon in phylogenetic context.

MATERIAL AND METHODS

Our study employed analyses of mitochondrial gene sequences as well as standard morphological comparisons. The specimens examined and tissues used for this study belong to the following collections:

AMNH, AMCC	American Museum of Natural History, New York, New York
ASNHC, ASK	Angelo State Natural History Collections, Angelo State University, San Angelo, Texas
CEBIOMAS	Centro de Ecología y Biodiversidad, Lima, Peru
CM	Carnegie Museum of Natural History, Pittsburgh, Pennsylvania
FMNH	Field Museum of Natural History, Chicago, Illinois
KU	Biodiversity Institute & Natural History Museum, University of Kansas, Lawrence, Kansas
LSUMZ, M	Museum of Natural Science, Louisiana State University, Baton Rouge, Louisiana
MUSA	Museo de Historia Natural, Universidad Nacional de San Agustín, Arequipa, Peru
MUSM	Museo de Historia Natural de la Universidad Nacional Mayor de San Marcos, Lima, Peru
MVZ	Museum of Vertebrate Zoology, University of California, Berkeley, California
QCAZ	Museo de Zoología of the Pontificia Universidad Católica del Ecuador, Quito, Ecuador
ROM	Royal Ontario Museum, Toronto, Ontario, Canada
TTU, TK	Museum of Texas Tech University, Lubbock, Texas
UMMZ	Museum of Zoology, University of Michigan, Ann Arbor, Michigan
USNM	National Museum of Natural History, Smithsonian Institution, Washington, D.C.

Morphological Analyses

We examined 102 specimens of adult *Hsunycteris* (56 males and 46 females; appendix 1) and evaluated external and osteological characters including, but not restricted to, those defined by Wetterer et al. (2000), Woodman and Timm (2006), and Dávalos et al. (2014). Dental homology nomenclature for the premolars in the discussions below follows that of Dávalos et al. (2014): 1st upper premolar (P4), 2nd upper premolar (P5), 1st lower premolar (p1), 2nd lower premolar (p4), and 3rd lower premolar (p5). All measurements reported herein are from adult individuals with closed epiphyses unless otherwise indicated. The first four measurements listed below were taken from skin labels or other records made by the original collector; all other measurements were taken by us using digital calipers and were recorded to the nearest 0.01 mm. Linear measurements are given in millimeters (mm), and weights are reported in grams (g). Descriptive statistics (mean and observed range) were calculated for all samples. Measurements are defined as follows:

Total length (TL): Distance from the tip of the snout to the tip of the last caudal vertebra.

Length of tail (LT): Measured from the point of dorsal flexure of the tail with the sacrum to the tip of the last caudal vertebra.

Hind-foot length (HF): Measured from the anterior edge of the base of the calcar to the tip of the claw of the longest toe.

Ear length (Ear): Measured from the ear notch to the fleshy tip of the pinna.

Forearm length (FA): Distance from the elbow (tip of the olecranon process) to the wrist (including the carpals). This measurement is made with the wing at least partially folded.

Greatest length of skull (GLS): Distance from the posteriormost point on the occiput to the anteriormost point on the premaxilla (excluding the incisors).

Condyloincisive length (CIL): Distance between a line connecting the posteriormost margins of the occipital condyles and the anteriormost point on the upper incisors.

Condylocanine length (CCL): Distance between a line connecting the posteriormost margins of the occipital condyles and a line connecting the anteriormost surface of the upper canines.

Braincase Breadth (BB): Greatest breadth of the globular part of the braincase, excluding mastoid and paraoccipital processes.

Width at Canines (C–C): Greatest breadth across the outer margins of the alveoli of upper canines.

Mastoid Process Width (MPW): Greatest breadth across the mastoid processes.

Maxillary Toothrow Length (MTRL): Distance from the anteriormost surface of the upper canine to the posteriormost surface of the crown of M3.

Width at M2 (M2–M2): Greatest width of palate across labial margins of the M2s.

Dentary Length (DENL): Distance from midpoint of condyle to the anteriormost point of the dentary.

Mandibular Toothrow Length (MANDL): Distance from the anteriormost surface of the lower canine to the posteriormost surface of m3.

Coronoid Height (COH): Perpendicular height from the ventral margin of mandible to the tip of the coronoid process.

All measurements were log-transformed to achieve normalization for statistical analyses. We evaluated differences between sexes and among species by principal component analysis (PCA) using a correlation matrix. Components with eigenvalues greater than 1 were retained. Principal component (PC) scores were plotted to show relationships between species groups in morphospace. Analyses were performed using PAST v3.01 (Hammer et al., 2001). We constructed a dichotomous identification key for all of the named species of *Hsunycteris* based on morphological traits identified during the course of the study.

Molecular Analyses

Field-collected frozen muscle and liver tissues preserved in EtOH of specimens cataloged as *Lonchophylla mordax*, *L. pattoni*, and *L. thomasi* were obtained for genetic analysis. DNA was extracted from small pieces of tissue (~5–10 mg) for each specimen using standard pro-

TABLE 1. Species, tissue/collection number, locality information, and GenBank accession numbers for the *Hsunycteris* and outgroup samples used in the molecular portion of this study.

Taxon	Tissue/Collection Numbers[a]	Locality[b]	GenBank
Glossophaga soricina	TK 104054/TTU 84826	Ecuador: Pastaza (22)	KF815298 [d]
Lionycteris spurrelli	TK 22540/TTU 39123	Panama: Darién (29)	KF815283 [d]
Lionycteris spurrelli	TK 22550/TTU 39129	Panama: Darién (29)	KF815284 [d]
Lionycteris spurrelli	TK 22549/TTU 39128	Panama: Darién (29)	KF815304 [d]
Platalina genovensium	TK 161667/MUSA 9383	Peru: Arequipa (32)	KF815311 [d]
Xeronycteris vieirai	MVZ 186020	Brazil: Paraiba (10)	KF815312 [d]
Lonchophylla chocoana	ROM 105786	Ecuador: Esmeraldas (13)	AF423092 [c]
Lonchophylla concava	TK 104601/QCAZ 9087	Ecuador: Esmeraldas (16)	KF815280 [d]
Lonchophylla concava	TK 104602/QCAZ 9568	Ecuador: Esmeraldas (16)	KF815281 [d]
Lonchophylla concava	TK 104612/QCAZ 9088	Ecuador: Esmeraldas (17)	KF815305 [d]
Lonchophylla concava	TK 135677/TTU102960	Ecuador: Esmeraldas (14)	KF815282 [d]
Lonchophylla handleyi	TK 22611/TTU 46169	Peru: Huánuco (33)	KF815285 [d]
Lonchophylla hesperia	M921/LSUMZ 27253	Peru: Lambayeque (34)	KF815310 [d]
Lonchophylla orienticollina	ASK 7733/QCAZ 8566	Ecuador: Morona Santiago (19)	KF815291 [d]
Lonchophylla orienticollina	ASK 7737/QCAZ 8570	Ecuador: Morona Santiago (19)	KF815308 [d]
Lonchophylla robusta	QCAZ 5406	Ecuador: Pichincha (24)	KF815313 [d]
Lonchophylla robusta	TK 104594/TTU 85366	Ecuador: Esmeraldas (16)	KF815286 [d]
Lonchophylla robusta	TK 104600/QCAZ 9085	Ecuador: Esmeraldas (16)	KF815287 [d]
Lonchophylla robusta	TK 104619/TTU 85391	Ecuador: Esmeraldas (17)	KF815306 [d]
Lonchophylla robusta	TK 135515/QCAZ 9091	Ecuador: Esmeraldas (14)	KF815288 [d]
Lonchophylla robusta	TK 135516/QCAZ 9092	Ecuador: Esmeraldas (14)	KF815289 [d]
Lonchophylla robusta	TK 135658/TTU 102941	Ecuador: Esmeraldas (14)	KF815290 [d]
Hsunycteris cadenai	TK 135800/QCAZ 9097	Ecuador: Esmeraldas (15)	KF815297 [d]
Hsunycteris cadenai	TK 104675/QCAZ 9096	Ecuador: Esmeraldas (18)	KF815307 [d]
Hsunycteris cadenai	TK 104676/TTU 85448	Ecuador: Esmeraldas (18)	KF815295 [d]
Hsunycteris cadenai	TK 104679/TTU 85451	Ecuador: Esmeraldas (18)	KF815296 [d]
Hsunycteris dashe	AMCC 109488/MUSM 15206	Peru: Loreto (35)	MF062529 [e]
Hsunycteris dashe	AMCC 109608/AMNH 273165	Peru: Loreto (35)	MF062528 [e]
Hsunycteris pattoni	AMNH 209358	Bolivia: Beni (1)	AF423084 [c]
Hsunycteris pattoni	AMNH 278465	Peru: Loreto (39)	MF062534 [e]
Hsunycteris pattoni	AMNH 278500	Peru: Loreto (39)	MF062533 [e]
Hsunycteris pattoni	AMCC 109525/AMNH 273069	Peru: Loreto (35)	MF062532 [e]
Hsunycteris pattoni	AMCC 109557/AMNH 273093	Peru: Loreto (35)	MF062531 [e]
Hsunycteris pattoni	CEBIOMAS 100	Peru: Loreto (39)	MF062536 [e]
Hsunycteris pattoni	CEBIOMAS 101	Peru: Loreto (39)	MF062537 [e]
Hsunycteris pattoni	KU 144232/MUSM 24350	Peru: Madre de Dios (42)	KF815314 [d]
Hsunycteris pattoni	AMCC 109713/MUSM 13205	Peru: Loreto (35)	MF062530 [e]

Taxon	Tissue/Collection Numbers[a]	Locality[b]	GenBank
Hsunycteris pattoni	AMCC 109527/MUSM 15207	Peru: Loreto (35)	MF062535 [e]
Hsunycteris pattoni	MVZ 192651/UMMZ 160710	Peru: Madre de Dios (41)	KF815309 [d]
Hsunycteris thomasi	KU 158056	Peru: Loreto (40)	KF815292 [d]
Hsunycteris thomasi	KU 158058	Peru: Loreto (40)	KF815315 [d]
Hsunycteris thomasi	TK104012/TTU 84784	Ecuador: Pastaza (21)	KF815293 [d]
Hsunycteris thomasi	AMCC 110340/AMNH 267940	French Guiana: Cayenne (25)	MF062539 [e]
Hsunycteris thomasi	AMCC 110262/AMNH 267943	French Guiana: Cayenne (25)	AF423086 [c]
Hsunycteris thomasi	KU 155154	Guyana: Potaro-Siparuni (27)	KF815294 [d]
Hsunycteris thomasi	TK 10310/CM 63723	Surinam: Nickerie (45)	KF815299 [d]
Hsunycteris thomasi	TK 10425/CM 63713	Surinam: Brokopondo (43)	KF815300 [d]
Hsunycteris thomasi	TK 17530/CM 76778	Surinam: Brokopondo (44)	KF815301 [d]
Hsunycteris thomasi	TK 17539/CM 76779	Surinam: Brokopondo (44)	KF815302 [d]
Hsunycteris thomasi	TK 19267/CM 78396	Venezuela: Bolívar (56)	KF815303 [d]

[a] Alphanumeric identifiers used by institutional tissue collections (and to label terminal in accompanying tree; fig. 6). See Material and Methods for names of museum collections identified by abbreviations in this table.
[b] Country and next-largest administrative unit (stated, department, province, etc.). Numbers in parentheses refer to gazetteer entries (appendix 2), which provide additional geographic information.
[c] Dávalos and Jansa (2004).
[d] Parlos et al. (2014).
[e] This study.

tocols of the QIAmp DNA Micro Kit (QIAGEN, Valencia, CA). Genomic DNA extractions were used as a template in polymerase chain reactions (PCR) to amplify the mitochondrial gene cytochrome *b* (*Cyt-b*, 1140 bp). Primers used in PCR amplification of *Cyt-b* were MVZ05 and UMMZ04 (Jansa et al., 1999). We integrated a series of overlapping 200 bp fragments (primers BATL4, BATH4, BATL5, and BATH5) from Dávalos and Jansa (2004) to improve the confidence of the sequence reads.

Polymerase chain reactions (PCR) were performed in a total volume of 25μl using DreamTaq polymerase mix (Thermo-Fisher Scientific, Waltham, MA), 1μl of each primer at 0.1μM, and 1μl of template DNA. Thermal cycler conditions to amplify *Cyt-b* consisted of an initial denaturation of 95°C for 10 min, followed by 35 cycles of denaturation at 95° C for 20 s, annealing at 48° C for 40 s, and elongation at 72° C for 1 min, and a final elongation step at 72° C for 10 min. PCR products were purified using ExoSAP-IT (USB Corporation, Cleveland, OH). Standard sequencing reactions were carried out at the Sackler Institute of Comparative Genomics (section 19) at American Museum of Natural History following ABI Prism BigDye Terminator cycle sequencing protocols (Applied Biosystems, Foster City, CA). All sequences were annotated, aligned, and contigs assembled in Geneious R8 v8.1.8 (www.geneious.com; Kearse et al., 2012).

Phylogenetic analyses were performed by combining the full *Cyt-b* sequences produced in this study with full and partial sequences available in GenBank from Dávalos and Jansa (2004) and Parlos et al. (2014; table 1). We determined the best-fit model of nucleotide substitution using the Akaike Information Criterion (AIC) in jModelTest v2.1 (Posada, 2008).

Model selection resulted in HKY+I+G, which we implemented in Bayesian and Maximum Likelihood (ML) phylogenetic analyses rooted using a sequence of *Glossophaga soricina* (TK 104054) as outgroup.

Bayesian phylogeny estimation was performed using MrBayes v3.2 (Ronquist et al., 2012) consisting of two independent runs of Metropolis-coupled Markov-chain Monte Carlo (MCMC) with four Markov chains. Each run was set for 10 million generations and sampling trees every 1000 generations. The average standard deviation of split frequencies was 0.008, indicating convergence of the analysis. Further assessment of stationarity was performed in Tracer v1.6 (Rambaut and Drummond, 2007) by examining log likelihood (ln L) scores. The first 20% of the estimated topologies were discarded as burn-in and a consensus Bayesian tree was constructed.

Maximum-likelihood (ML) analysis was performed using Garli v2.1(Bazinet et al., 2014). Parameter settings included a heuristic search of four replicates over 5×10^6 generations and a ML starting tree inferred from stepwise addition sequence. Other parameters were set as default. Nodal support for ML estimation was evaluated using 100 replicates of nonparametric bootstrap analysis. A majority-rule consensus tree of bootstrap replicates was constructed in the R package "ape" (analyses of phylogenetics and evolution) ver. 4.1 (Paradis, 2012).

Finally, we estimated average uncorrected (p) and K2P pairwise distances using the R package ape v4.1 (Paradis, 2012). We trimmed all sequences in this analysis to the length of the shortest sequence (400 bp). These estimates were used to compare genetic distances of specimens collected within the Yavarí-Ucayali interfluvial region, and between these and other previously defined *Hsunycteris* groups in Parlos et al. (2014).

SYSTEMATICS

Family Phyllostomidae Gray, 1825

Subfamily Lonchophyllinae Griffiths, 1982

Tribe Hsunycterini Parlos et al., 2014

Genus *Hsunycteris* Parlos et al., 2014

Hsunycteris dashe, new species

Dashe's nectar-feeding bat

Lonchophylla mordax: Fleck et al., 2002: 96.
Hsunycteris sp. nov.: Voss et al., 2016: 11.

Holotype: The holotype (MUSM 15206; figs. 1, 3A, 4A), an adult female specimen preserved in alcohol with the skull removed and cleaned, was collected by David W. Fleck (original number: DWF 380) on 2 September 1999 at Nuevo San Juan (73°9′50″W, 5°14′50″S; 150 m above sea level), a Matses village on the right (SE) bank of the Río Gálvez in the Peruvian department of Loreto (fig. 2). Frozen tissues are deposited at the Ambrose Monell Cryo Collection of the American Museum of Natural History (AMCC 109488).

FIGURE 1. Dorsal and ventral views of the cranium and lateral view of the cranium and mandible of *Hsunycteris dashe* (MUSM 15206, holotype). Scale bar = 5 mm.

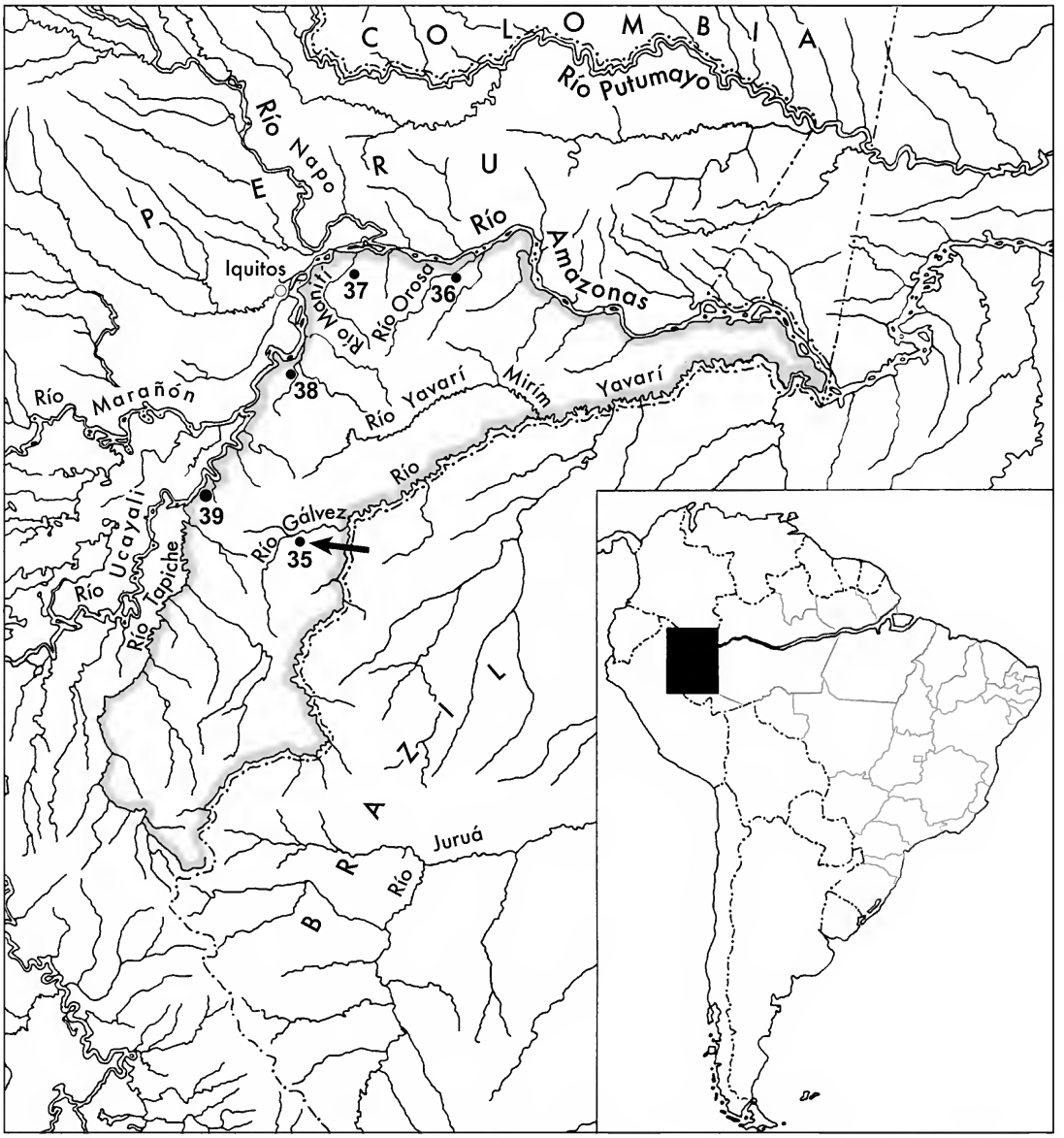

FIGURE 2. Map showing collecting localities of *Hsunycteris* species within the Yavarí-Ucayali interfluvial region (boundaries highlighted in gray). See appendix 2 for locality names and geographic coordinates. The arrow indicates the type locality of *H. dashe*.

Paratypes: Two additional specimens, a lactating adult female (AMNH 273165 [DWF 662]) and her female pup (MUSM 15211 [DWF 663]), were collected at the type locality by David W. Fleck on 21 October 1999. The adult paratype (AMNH 273165), preserved in alcohol with the skull removed and cleaned, is accompanied by frozen tissues deposited at the Ambrose Monell Cryo Collection of the American Museum of Natural History (AMCC 109608). The juvenile paratype (MUSM 15211) is preserved in alcohol.

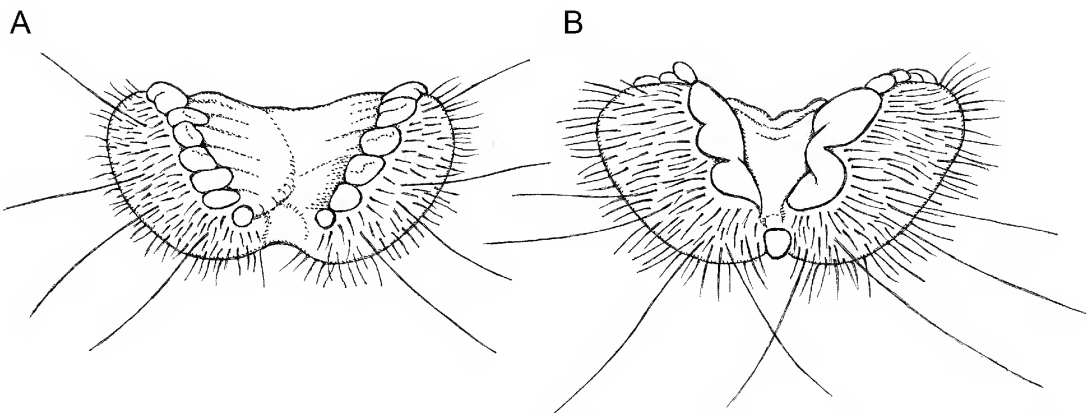

FIGURE 3. Anterior views of the chins of *Hsunycteris dashe* (**A**, AMNH 273165) and *H. pattoni* (**B**, MUSM 13205) illustrating taxonomic differences in the arrangement of the dermal papillae. In *H. dashe* the chin has several small dermal papillae arranged in a V and separated by a wide basal cleft. In *H. pattoni*, however the dermal papillae on the chin are larger and are not separated by a basal cleft.

Distribution: *Hsunycteris dashe* is known only from the vicinity of the type locality in the Yavarí-Ucayali interfluvial region of the Peruvian Amazon (fig. 2).

Diagnosis and Description: *Hsunycteris dashe* is the largest species in the genus (FA 35–36 mm; tables 2–3). Dorsal pelage 9–10 mm long, fur distinctly bicolored with pale pinkish bases (20% of length) and pale brown tips; ventral pelage 7 mm long, similar in color to the dorsal pelage, bicolored with pale pinkish bases (30% of length) and pale brown tips. Two interramal vibrissae present; genal vibrissae absent. Central rib of noseleaf weakly defined from lateral portions, extending from apex to edge of upper lip. Chin with several small dermal papillae arranged in a V shape and separated by a wide cleft (fig. 3A). Antero-internal surface of pinna sparsely covered with long hairs. Dorsal surface of the forearm naked. Metacarpal formula III > V > IV. Dorsal surface of uropatagium naked. Dorsal surface of foot sparsely covered by short hairs.

Skull with broad rostrum; postorbital region not inflated and lacking lateral projections (fig. 1). Lateral margin of infraorbital foramen not projecting beyond rostral outline in dorsal view. Sphenoidal crest (Giannini et al., 2006: fig. 10) well developed. Posterior border of hard palate V-shaped. Left and right basisphenoid pits separated by narrow septum. Dentary deep, coronoid process low (slightly above level of articular condyle), and angular process broad.

Dental formula I2/2, C1/1, P2/3, M3/3 × 2 = 34 or I2/2, C1/1, P3/3, M3/3 × 2 = 36.[3] Inner and outer upper incisors not in contact. Outer upper incisors relatively large. P4 lingual cusp absent; P5 lingual cusp weakly developed; small gap present between P5 and M1 (fig. 4A). M1 parastyle well developed and labially oriented; M1 and M2 with broad protocone basin; M3 large; palate posterior to M3 shorter than the length of M3 (figs. 1, 4A).

[3] The former dental formula characterizes the adult paratype, and it is the usual formula in other congeneric species, whereas the holotype has an additional pair of small upper premolars (figs. 1, 4A). With only two adult specimens in hand, it is obviously impossible to determine which formula predominates in the species, although we suspect that the small anterior premolars of the holotype are supernumerary teeth, which commonly occur in other lonchophyllines (Phillips, 1971; Nogueira et al., 2014).

TABLE 2. Measurements (mm) and weights (g) of the type series of *Hsunycteris dashe*.

	MUSM 15206♀[a]	AMNH 273165♀[b]	MUSM 15211♀[b, c]
TL	61.0	65.0	45.0
LT	12.0	8.0	5.0
HF	11.0	10.0	9.0
Ear	13.0	14.0	10.0
FA	35.0	36.0	23.0
GLS	20.8	20.5	–
CIL	19.8	19.8	–
CCL	18.9	18.9	–
BB	8.7	8.5	–
C–C	4.0	4.0	–
MPW	8.9	8.9	–
MTRL	6.4	6.5	–
M2–M2	5.5	5.5	–
DENL	13.6	13.7	–
MANDL	6.8	6.8	–
COH	3.6	3.8	–
Weight	9.3	10.2	3.7

[a] Holotype.
[b] Paratype.
[c] Juvenile, pup of AMNH 273165.

Lower incisors large and broad. Distal cusp weakly developed on p1. Anterior cusp of p4 oriented horizontally. Protoconid labially oriented on m1; m1 paracristid notch strongly developed. Hypoconid wide on m2.

Comparisons: External and craniodental measurements for *Hsunycteris dashe* and other congeneric species are provided in tables 2 and 3. *Hsunycteris dashe* can be easily distinguished from all other species of *Hsunycteris* by its longer forearm. However, there is substantial overlap among all *Hsunycteris* species in craniodental measurements, with *H. dashe* falling at the larger end of the spectrum for most variables.

Externally, *Hsunycteris dashe* is distinguished from all other species in the genus by having longer hairs between the shoulders (9–10 mm, versus 7–8 mm in *H. cadenai*, *H. pattoni*, and *H. thomasi*). The central rib of the noseleaf extends from the tip of the spear to the edge of the upper lip in *H. dashe* and *H. thomasi*, and it is weakly defined from the lateral portions of the noseleaf. In contrast, the central rib of the noseleaf is well defined but does not reach the edge of the upper lip in *H. pattoni*, and a distinct central rib is absent in *H. cadenai*. The chin has several small dermal papillae arranged in a V and separated by a wide basal cleft in *H. dashe* (fig. 3A), whereas the dermal papillae are larger and not separated by a basal cleft in *H. cadenai*, *H. pattoni*, and *H. thomasi* (fig. 3B). The antero-internal surface of each pinna is sparsely covered with long hairs in *H. dashe*, *H. cadenai*, and *H. thomasi*, whereas these hairs are more abundant in *H. pattoni*. Lastly,

TABLE 3. Measurements (mm) and weights (g) of three species of *Hsunycteris*.

	H. cadenai		*H. pattoni*		*H. thomasi*	
	Females[a]	Males[b]	Females[c]	Males[d]	Females[e]	Males[f]
TL	62 (59–65) 2	61, 60	60 (50–67) 17	59 (50–68) 19	58 (49–65) 18	59 (53–64) 29
LT	8 (7–9) 2	10, 8	8 (5–10) 16	7 (5–9) 19	6 (4–9) 18	7 (4–11) 29
HF	8 (8) 5	10, 8	9 (7–11) 17	9 (8–10) 19	9 (7–11) 17	9 (7–11) 30
Ear	14 (14) 2	14, 15	15 (12–17) 17	14 (12–16) 19	15 (11–16) 18	15 (12–18) 28
FA	32.1 (31.6–32.7) 5	31.0, 31.0	32.8 (31.0–34.0) 17	32.0 (31.0–34.0) 19	32.3 (30.6–34.3) 18	31.7 (29.7–33.5) 32
GLS	21.1 (20.7–21.7) 3	21.2, 21.3	20.8 (19.9–21.8) 14	20.6 (19.7–21.1) 9	20.7 (19.6–21.7) 17	20.8 (19.7–21.9) 33
CIL	20.6 (20.2–20.9) 2	20.1, 20.6	20.2 (19.2–21.2) 12	20.0 (19.4–20.4) 9	19.9 (18.8–20.8) 16	20.1 (19.1–21.1) 31
CCL	19.5 (19.1–19.8) 2	19.0, 19.5	19.2 (18.4–20.2) 12	19.1 (18.5–19.8) 9	18.9 (17.9–19.7) 17	19.1 (18.1–20.1) 33
BB	8.6 (8.4–9.0) 3	8.8, 8.7	8.2 (7.9–8.5) 14	8.4 (8.2–8.6) 9	8.2 (7.7–8.7) 18	8.3 (8.0–8.6) 33
C–C	3.8 (3.7–3.9) 4	3.9, 4.0	3.7 (3.5–3.9) 11	3.7 (3.6–3.8) 9	3.7 (3.4–4.1) 17	3.8 (3.5–4.2) 31
MPW	9.1 (9.1) 3	9.1, 9.3	8.7 (8.2–9.4) 14	8.8 (8.5–8.9) 9	8.5 (8.0–8.8) 17	8.7 (8.3–9.0) 33
MTRL	6.8 (6.7–6.9) 3	6.9, 7.0	6.9 (6.5–7.3) 12	6.7 (6.5–7.2) 9	6.6 (6.3–7.1) 18	6.7 (6.1–7.2) 33
M2–M2	5.1 (5.0–5.3) 3	5.4, 5.3	5.3 (5.0–5.7) 14	5.2 (4.9–5.5) 9	5.1 (4.8–5.3) 16	5.2 (4.9–5.7) 32
DENL	14.4 (14.1–14.5) 3	14.0, 14.5	14.2 (13.5–15.0) 13	14.1 (13.8–14.6) 9	13.9 (13.0–14.7) 15	14.2 (13.4–14.9) 32
MANDL	7.2 (7.1–7.3) 3	7.2, 7.5	7.2 (6.9–7.5) 13	7.1 (6.8–7.9) 9	6.9 (6.6–7.3) 16	7.1 (6.8–7.6) 32
COH	3.9 (3.7–4.0) 3	4.0, 4.0	3.5 (3.0–3.9) 14	3.6 (3.3–3.9) 9	3.5 (3.1–4.0) 16	3.7 (3.3–4.0) 32
Weight	––	–, –	7.9 (5.0–15.0) 16	6.5 (3.0–8.5) 17	6.2 (5.0–9.0) 16	6.5 (5.1–9.0) 24

[a] Summary statistics (mean, observed range in parentheses, and sample size) for measurements of USNM 338726, 446481, 446482, 483363, 483364.

[b] USNM 483359 (holotype), 483365.

[c] Summary statistics (mean, observed range in parentheses, and sample size) for measurements of AMNH 209358, 273093, 273126, 278465, 278500; CEBIOMAS 100; MUSM 863, 5589, 5932, 13205, 15209, 21173, 24350 (holotype); USNM 530962, 549362, 549363, 584475.

[d] Summary statistics (mean, observed range in parentheses, and sample size) for measurements of AMNH 273069, 273124; CEBIOMAS 101; MUSM 5523, 5541, 5542, 5933, 5940, 15207, 15208, 15210, 31927–31930; USNM 530960, 530961, 549364, 584474.

[e] Summary statistics (mean, observed range in parentheses, and sample size) for measurements of FMNH 87070; MUSM 21172; USNM 335180, 393014, 407797–407799, 407802, 460097, 528325, 549366, 549367, 574511, 575486, 575488, 575497, 582300, 582301.

[f] Summary statistics (mean, observed range in parentheses, and sample size) for measurements of AMNH 16120 (holotype), 267940, 267943; MUSM 5509, 5931, 21170, 21171; USNM 306582, 361570, 361571, 385753, 393013, 407796, 407801, 407803, 415387, 415388, 456537, 460098, 530958, 530959, 549369, 559186, 560560, 574510, 575489–575491, 575493, 575494, 575496, 575498, 582299.

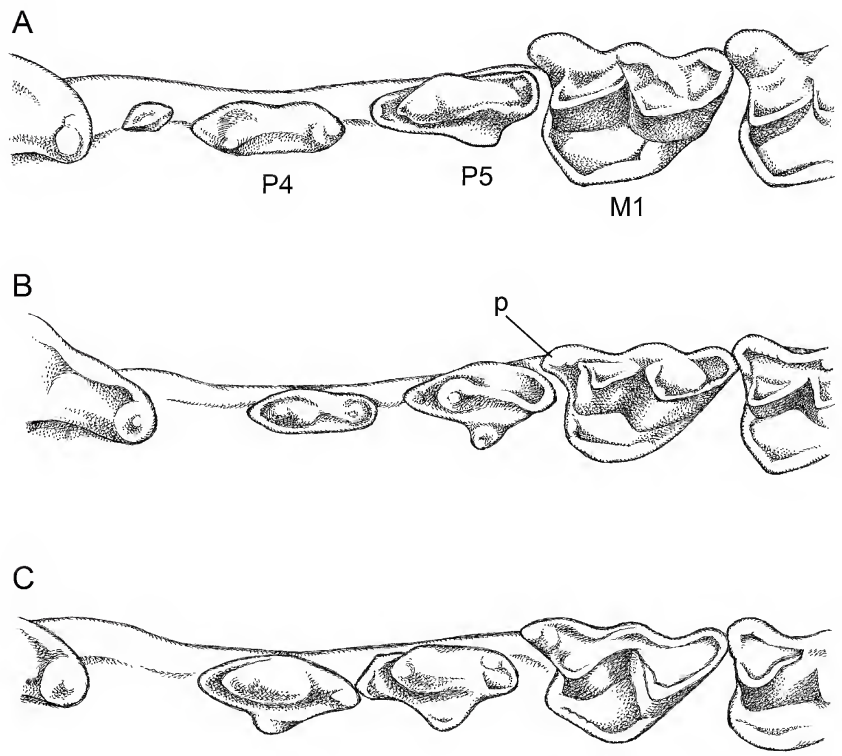

FIGURE 4. Occlusal views of partial upper toothrows in *Hsunycteris dashe* (**A**, MUSM 15206), *H. pattoni* (**B**, MUSM 13205), and *H. thomasi* (**C**, AMNH 16120) illustrating taxonomic differences in the morphology of the premolars and first molar (see text). Abbreviations: **p,** parastyle of M1; **P4,** first upper premolar; **P5,** second upper premolar; **M1,** first upper molar.

metacarpal V is longer than metacarpal IV in *H. dashe*, whereas metacarpal V is shorter than IV in *H. cadenai* and *H. pattoni*, and these metacarpals are subequal in length in *H. thomasi*.

The skull of *Hsunycteris dashe* is distinguished from those of all other species in the genus by having a relatively broader rostrum and lacking inflation of the postorbital region (versus rostrum narrower and postorbital region inflated in *H. cadenai*, *H. pattoni*, and *H. thomasi*). The postorbital region lacks a lateral projection in *H. dashe*, *H. pattoni*, and *H. thomasi*, whereas a lateral projection is present in *H. cadenai* (see Woodman and Timm, 2006: fig. 11A). The lateral margin of the infraorbital foramen does not project beyond rostral outline in dorsal view in *H. dashe*, whereas the infraorbital foramen is wider with a lateral margin that projects beyond rostral outline in dorsal view in *H. cadenai*, *H. pattoni*, and *H. thomasi*. The sphenoidal crest is well developed in *H. dashe*, whereas this crest is weakly developed in *H. cadenai*, *H. pattoni*, and *H. thomasi*. The septum separating the left and right basisphenoid pits is narrow in *H. dashe* and *H. pattoni*, whereas the septum is broader in *H. cadenai*.[4] The maxilla imme-

[4] *Hsunycteris thomasi* exhibits considerable intraspecific variation in this feature, with some specimens having a relatively narrow septum (e.g., AMNH 267940) and others having a broader septum (e.g., AMNH 16120).

diately posterior to M3 is less than the length of M3 in *H. dashe*, *H. cadenai*, and *H. pattoni*; in contrast, the maxilla posterior to M3 is longer than the length of M3 in *H. thomasi*.

The body of the dentary is deep in *Hsunycteris dashe*, *H. cadenai*, and *H. thomasi*, whereas it is shallow and the entire dentary appears more slender in *H. pattoni*. The coronoid process is low (extending dorsally slightly above the level of the articular condyle) in *H. dashe* and *H. thomasi*, whereas the coronoid process is significantly higher in *H. cadenai* and *H. pattoni*. The angular process is broad in *H. dashe*, *H. cadenai*, and *H. thomasi*, whereas it is narrower in *H. pattoni*.

In lateral view, the inner and outer upper incisors are not in contact in *Hsunycteris dashe*, whereas these teeth are in contact in *H. cadenai* and *H. pattoni* (*Hsunycteris thomasi* exhibits variation in this character: the inner and outer upper incisors are in contact in some specimens [e.g., AMNH 16120] but not in others [e.g., AMNH 267940, 267943]). The outer upper incisors are large (slightly smaller than inner upper incisors) in *H. dashe* whereas they are proportionally smaller (less than half the size of the inner upper incisors) in *H. cadenai*, *H. thomasi*, and *H. pattoni*. Whereas P4 lacks a lingual cusp in *H. dashe* (fig. 4A), *H. cadenai*, and *H. pattoni* (fig. 4B), this cusp is present in *H. thomasi* (fig. 4C). The lingual cusp of P5 is weakly developed in *H. dashe* (fig. 4A), whereas this cusp is well developed and narrow in *H. pattoni* (fig. 4B) and well developed and broad in *H. cadenai* and *H. thomasi* (fig. 4C). There is a small gap present between P5 and M1 in *H. dashe*, *H. cadenai*, and *H. pattoni*, whereas this gap is variable *H. thomasi* (e.g., present and wide in AMNH 16120, but absent in AMNH 267940 and 267943). The parastyle on M1 is well developed and labially oriented in *H. dashe*. In contrast, the parastyle is weakly developed and directed anteriorly in *H. cadenai*, while it is well developed and directed anteriorly in *H. pattoni* and *H. thomasi*. The protocone basins of M1 and M2 are broad in *H. dashe* and *H. thomasi*, whereas they are reduced in *H. cadenai* and *H. pattoni*. The third upper molar is large in *H. dashe*, *H. cadenai*, *H. pattoni*, and some specimens of *H. thomasi* (e.g., AMNH 267940, 267943), whereas other specimens of *H. thomasi* have smaller M3s (e.g., AMNH 16120).

The lower incisors are large and mesiodistally broad in *Hsunycteris dashe* and *H. cadenai*, whereas these teeth are proportionally smaller and narrower in *H. thomasi* and *H. pattoni*. The distal cusp on p1 is weakly developed in *H. dashe*, whereas it is well developed in *H. cadenai*, *H. pattoni*, and *H. thomasi*. The anterior cusp of p4 is oriented horizontally in *H. dashe*, whereas this cusp in *H. cadenai* and *H. pattoni* is inclined upwards. *Hsunycteris thomasi* exhibits intraspecific variation in this feature, with some individuals having the cusp oriented horizontally (e.g., AMNH 267940, 267943) while it is inclined upwards in others (e.g., AMNH 16120). The paracristid notch of m1 is strongly developed in *H. dashe* and *H. cadenai*, but this notch is weakly developed or absent in *H. pattoni* and *H. thomasi*. The hypoconid of m2 is wide in *H. dashe* and *H. cadenai*, whereas it is narrow in *H. thomasi* and *H. pattoni*.

Morphometric Analyses: Our multivariate statistical analysis included only female specimens because males are unknown for *Hsunycteris dashe*. We compared three specimens of *H. cadenai*, 14 of *H. pattoni*, 18 of *H. thomasi*, and two of *H. dashe* (appendix 1), using a principal components analysis (PCA) based on one external measurement (FA) and the 11 craniodental measurements described above. The first three principal components accounted for 82.4% of the

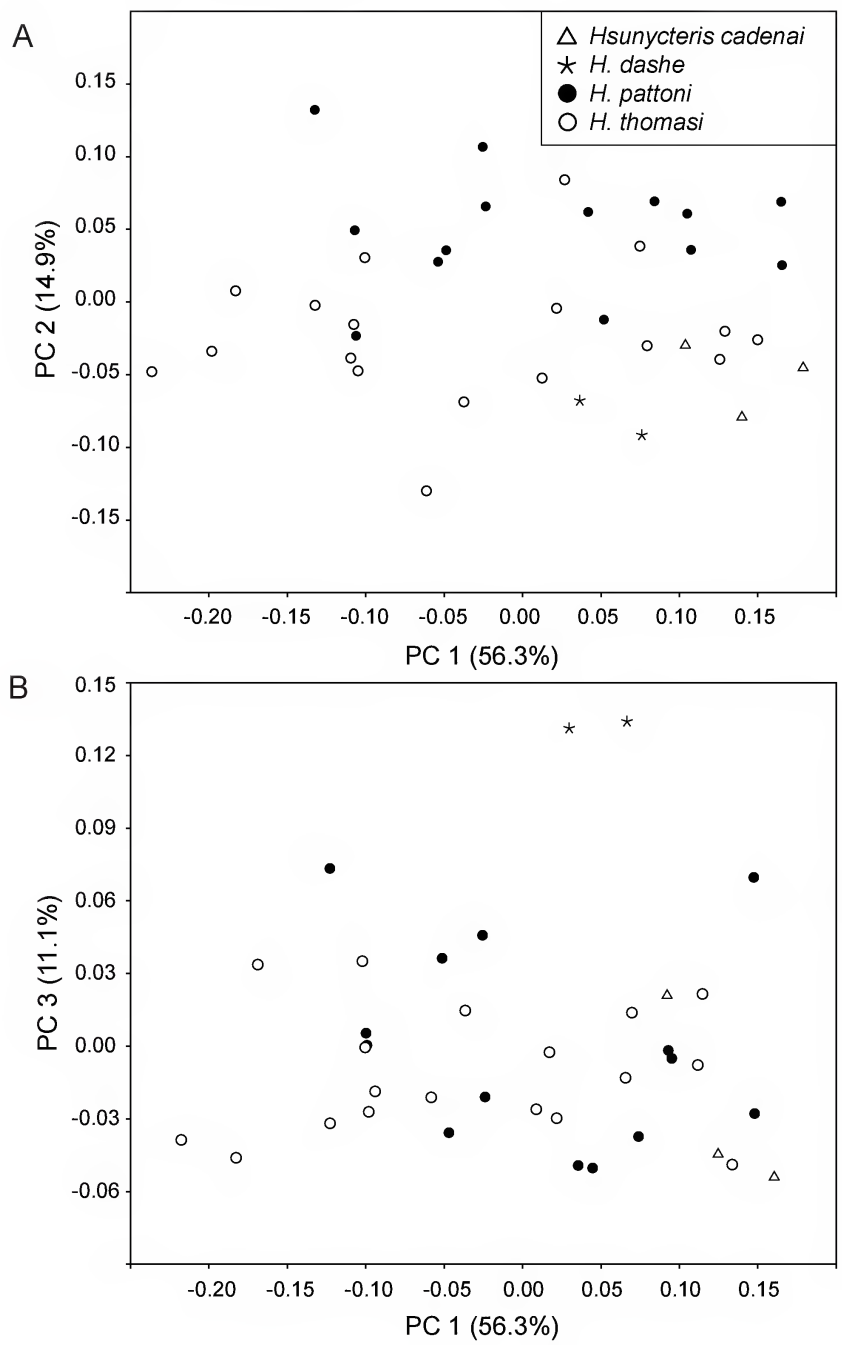

FIGURE 5. Results of principal components analysis, illustrating the dispersion of specimen scores for female *Hsunycteris cadenai* (open triangles), *H. dashe* (asterisk), *H. pattoni* (filled circles), and *H. thomasi* (open circles). See text for explanation and appendix 3 for factor loadings and other results.

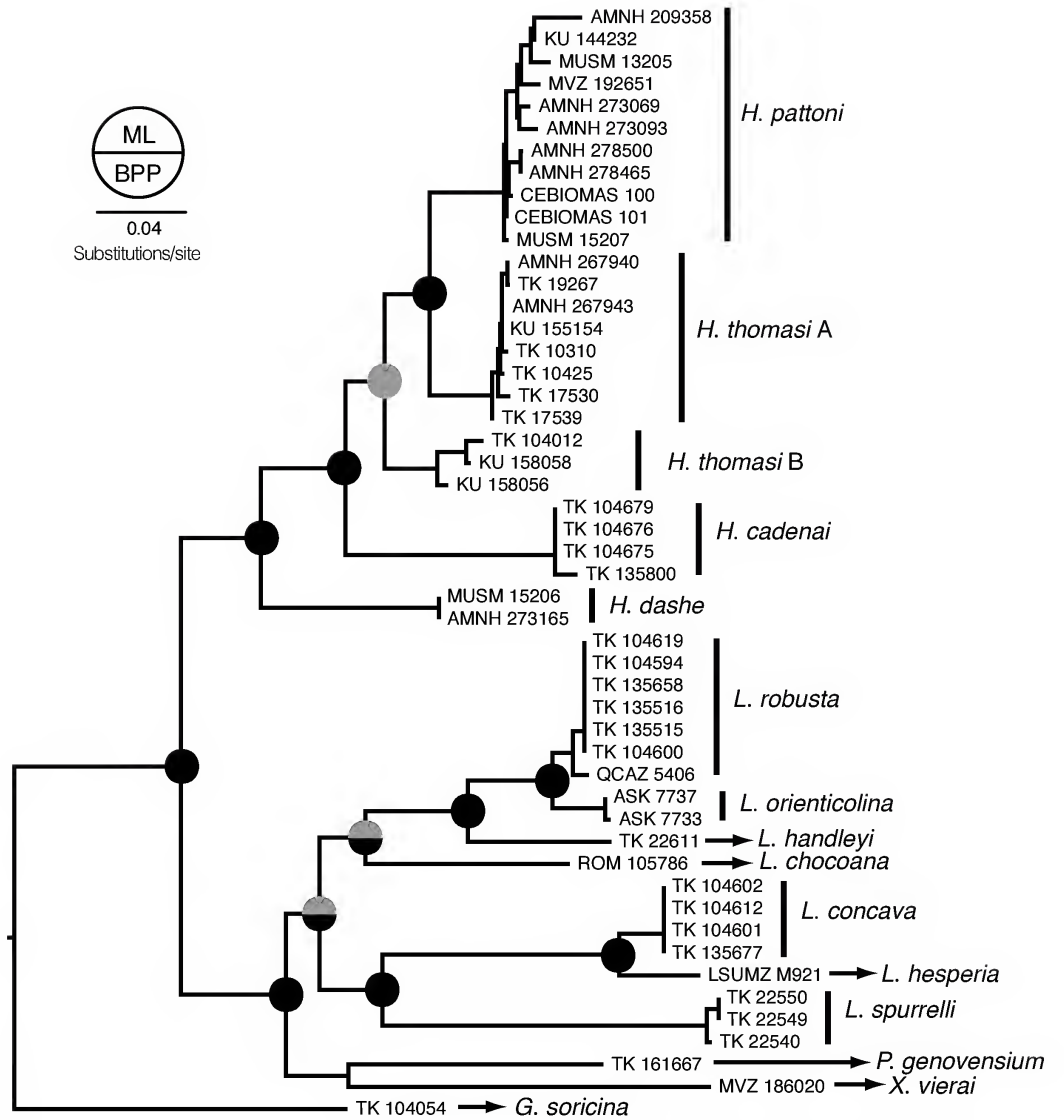

FIGURE 6. Cytochrome-*b* maximum likelihood (ML) phylogram for the subfamily Lonchophyllinae. Support statistics from ML analysis and Bayesian inference (BI) are indicated at each resolved node. For the ML analysis, gray shading indicates bootstrap frequencies between 50% and 75% and black indicates bootstrap frequencies >75%. For the BA, gray indicates posterior probabilities <0.95, whereas black indicates posterior probabilities >0.95.

total variance in the log-transformed measurements of this material (appendix 3). PC 1 accounted for the highest percentage (56.3%), and this vector has uniformly positive loadings, suggesting that it is a size factor (with a notably high loading for coronoid height). Although all four species show overlapping scores on PC1 and PC2 (fig. 5A), *H. dashe* specimens are widely separately from the other three species on PC3 (fig. 5B). Factor loadings on PC3 suggest that this separation is attributable primarily to differences in forearm length, width at canines, and width at M2.

FIGURE 7. Dashe, the Matses hero who led his people to victory in their struggle for survival during the mid-20th century. (Photographed by Steven Romanoff on the upper Chobayacu, ca. 1975.)

Molecular Analyses: Molecular analysis of mitochondrial *Cyt-b* sequences from selected specimens (table 1) recovered well-supported clades consistent with the divergence of *Hsunycteris* from other lonchophyllines (fig. 6). The monophyly of *Hsunycteris* is strongly supported by these data, and *H. dashe* was recovered as the sister lineage of a robustly supported clade comprised of *H. cadenai*, *H. pattoni*, and *H. thomasi* in both Bayesian inference and ML analyses. Pairwise genetic comparisons between *H. dashe* and other congeneric species averaged at least 11% and 15% for uncorrected-p and K2P distances, respectively (appendix 4).

Natural History: Our three specimens of *Hsunycteris dashe* were all collected at diurnal roosts discovered by Matses hunters near Nuevo San Juan. The first to be collected (MUSM 15206, an adult female) was found roosting alone beneath the undercut bank of a small stream in dense valley-bottom primary forest on 2 September 1999. D.W.F. collected this bat after having been led to the roost by the hunters who found it. According to his field notes, "the roof of the [undercut] bank was held together by the root mass of a nearby tree," and the bat was hanging from this root-stabilized surface, about 1 m above the water's edge. The other two specimens (AMNH 273165, MUSM 15211; mother and young, respectively) were found roosting together with a third individual (which escaped capture) beneath the undercut bank of another stream, in primary upland forest on 21 October 1999. No additional details were provided by the Matses hunters who collected these two specimens and described their roost to D.W.F.

Except for the narrow floodplain of the Río Gálvez, the landscape surrounding Nuevo San Juan consists of low hills and terraces (nowhere more than 200 m above sea level) eroded from Miocene lake sediments; there are no caves or rock outcrops anywhere in the region. As described elsewhere, the average annual rainfall is probably close to 3000 mm. Except where cleared for Matses horticulture or regenerating from their slash-and-burn clearings, the local vegetation consists of a variety of primary formations determined by drainage and seasonal flooding (Fleck and Harder, 2000; Voss and Fleck, 2011). All our specimens of *Hsunycteris dashe* were taken in tall, undisturbed forest on hilly interfluvial terrain far from the palm swamps and seasonally flooded formations of the Gálvez floodplain.

Etymology: For Dashe (ca. 1910–1980, fig. 7), also known as Quioshash, a hero of the Matses people. Dashe grew up during the rubber boom, when mercenaries were sent to Matses territory to exterminate the indigenous inhabitants. Dashe grew up fleeing from attackers who killed his kinsmen and carried off women and children to be prostituted or sold as slaves. After he had grown to manhood, Dashe rallied the Matses to fight back, leading multiple successful raids on rubber camps and settlements, eventually expelling all outsiders (Jiménez Huanán et al., 2014). Without his courage and military cunning the Matses would no longer exist as an intact culture with legally recognized title to their tribal land.

DISCUSSION

With the description of *Hsunycteris dashe* the subfamily Lonchophyllinae now includes 20 species grouped in five genera, three of which are monotypic (Parlos et al., 2014; Moratelli and Dias, 2015). The type locality of *H. dashe* (fig. 2: locality 35), is one of the most diverse sites in the Neotropics, with over 60 bat species documented to date (Fleck et al., 2002; Voss et al., 2016). Only one other congener (*H. pattoni*) is known to occur at Nuevo San Juan, but a third species (*H. thomasi*) has been recorded at Jenaro Herrera (fig. 2: locality 39), only 70 km to the northwest. Both of these localities lie within the Yavarí-Ucayali interfluvial region. Accordingly, we expect that all three species (*H. dashe*, *H. pattoni*, and *H. thomasi*) likely occur sympatrically in this part of northeastern Peru. By contrast, *H. cadenai* is (insofar as known) a Trans-Andean species that is unlikely to occur with *H. dashe* (see Mantilla-Meluk et al., 2010).

The paraphyletic status of *Hsunycteris thomasi* was first reported by Parlos et al. (2014). Mitochondrial and nuclear markers support the grouping of *H. thomasi* specimens in two clades, one of which is more closely related to *H. pattoni* than the other (fig. 6). Confusingly, representatives of both clades of *H. thomasi* have been collected near the Venezuelan type locality (Parlos et al., 2014). In our morphological analyses we were unable to identify any morphological traits that unambiguously distinguish members of the two clades of *H. thomasi* recovered in our molecular analysis. To identify which of the two clades the name *H. thomasi* properly applies to, and which represents an undescribed taxon, we attempted to obtain sequence data from the holotype (AMNH 16120), a specimen that was collected in 1909. Unfortunately, our attempts to amplify mitochondrial fragments from the holotype have thus far been unsuccessful.

Key to the Species of *Hsunycteris*

1. Forearm ≥ 35.0 mm; hairs between the shoulders ≥9 mm; dermal papillae on chin arranged in a V and separated by a wide basal cleft; metacarpal V longer than metacarpal IV; rostrum broad; lateral margin of infraorbital foramen does not project beyond rostral outline in dorsal view; outer upper incisors large; P5 lingual cusp weakly developed ..... *Hsunycteris dashe*

1′. Forearm ≤34.5 mm; hairs between the shoulders ≤8 mm; dermal papillae on chin arranged in a V but not separated by a wide basal cleft; metacarpal V shorter than or subequal to metacarpal IV; rostrum narrow; lateral margin of infraorbital foramen does project beyond rostral outline in dorsal view; outer upper incisors small; P5 lingual cusp well-developed. 2

2. Postorbital region with a lateral projection; M1 parastyle weakly developed; lower incisors large and broad; m1 paracristid notch strongly developed; m2 hypoconid wide. . . . . *Hsunycteris cadenai*

2′. Postorbital region lacks a lateral projection; M1 parastyle well developed; lower incisors small and narrow; m1 paracristid notch weakly developed or absent; m2 hypoconid narrow 3

3. Metacarpal V shorter than metacarpal IV; extent of maxillary posterior to M3 less than the length of M3; dentary slender; angular process narrow; P4 lingual cusp absent; P5 lingual cusp narrow . . . . . *Hsunycteris pattoni*

3′. Metacarpal V subequal to metacarpal IV; extent of maxillary posterior to M3 greater than the length of M3; dentary deep; angular process broad; P4 lingual cusp present; P5 lingual cusp broad. . . . . *Hsunycteris thomasi*

ACKNOWLEDGMENTS

We are grateful to our Matses hosts and field assistants at Nuevo San Juan, where R.S.V. and D.W.F. collected bats in 1998 and 1999; to the Instituto Nacional de Recursos Naturales (INRENA), which issued the necessary collecting and export permits; and to the MUSM (especially Víctor Pacheco and Sergio Solari), which provided important logistical support in Lima. Our 1998/1999 field research at Nuevo San Juan was partially supported by grants from the AMNH Center for Biodiversity and Conservation. The following curators and collection staff graciously provided access to specimens under their care: Erika Paliza (CEBIOMAS); Bruce Patterson (FMNH), Víctor Pacheco (MUSM); and Alfred Gardner, Darrin Lunde, and Suzanne Peurach (USNM). Alfred Gardner and an anonymous reviewer provided helpful comments on the submitted draft of this manuscript. Patricia J. Wynne drew figures 2, 3, and 4. Alejandra Camacho provided information about Ecuadorean coordinates. We thank Steven Romanoff for permission to reproduce his photograph of Dashe.

REFERENCES

Allen, J.A. 1904. New bats from tropical America, with note on species of *Otopterus*. Bulletin of the American Museum of Natural History 20 (20): 227–237.

Bazinet, A.L., D.J. Zwickl, and M.P. Cummings. 2014. A gateway for phylogenetic analysis powered by grid computing featuring GARLI 2.0. Systematic Biology 63: 812–818.

Cirranello, A.L., N.B. Simmons, S. Solari, and R.J. Baker. 2016. Morphological diagnoses of higher-level phyllostomid taxa (Chiroptera: Phyllostomidae). Acta Chiropterologica 18: 39–71.

Clare, E.L., B.K. Lim, M.B. Fenton, and P.D.N. Hebert. 2011. Neotropical bats: estimating species diversity with DNA barcodes. PLoS ONE 6: e22648.

Dávalos, L.M., and S.A. Jansa. 2004. Phylogeny of the Lonchophyllini (Chiroptera: Phyllostomidae). Journal of Mammalogy 85: 404–413.

Dávalos, L.M., A.L. Cirranello, J.H. Geisler, and N.B. Simmons. 2012. Understanding phylogenetic incongruence: lessons from phyllostomid bats. Biological Reviews 87: 991–1024.

Dávalos, L.M., P.M. Velazco, O.M. Warsi, P.D. Smits, and N.B. Simmons. 2014. Integrating incomplete fossils by isolating conflictive signal in saturated and non-independent morphological characters. Systematic Biology 63: 582–600.

Fleck, D.W., and J.D. Harder. 2000. Matses Indian rainforest habitat classification and mammalian diversity in Amazonian Peru. Journal of Ethnobiology 20: 1–36.

Fleck, D.W., R.S. Voss, and N.B. Simmons. 2002. Underdifferentiated taxa and sublexical categorization: an example from Matses classification of bats. Journal of Ethnobiology 22: 61–102.

Giannini, N.P., J.R. Wible, and N.B. Simmons. 2006. On the cranial osteology of Chiroptera. I. *Pteropus* (Megachiroptera: Pteropodidae). Bulletin of the American Museum of Natural History 295: 1–134.

Griffiths, T.A., and A.L. Gardner. 2008. Subfamily Lonchophyllinae Griffiths, 1982. *In* A.L. Gardner, (editor), Mammals of South America, vol. 1: Marsupials, xenarthrans, shrews, and bats: 244–255. Chicago: University of Chicago Press.

Hammer, Ø., D.A.T. Harper, and P.D. Ryan. 2001. PAST: paleontological statistics software package for education and data analysis. Palaeontologia Electronica 4: 1–9.

Jansa, S.A., S.M. Goodman, and P.K. Tucker. 1999. Molecular phylogeny and biogeography of the native rodents of Madagascar (Muridae: Nesomyinae): a test of the single-origin hypothesis. Cladistics 15: 253–270.

Jiménez Huanán, D.M., Jiménez Ëshco, A., and D.W. Fleck. 2014. Matses icampid: ëndenquio icampid Manuel Tumi chuibanaid (La historia de los Matses, primera parte, 1860–1947: historia antigua según Manuel Tumí). Iquitos: Tierra Nueva.

Kearse, M., et al. 2012. Geneious basic: an integrated and extendable desktop software platform for the organization and analysis of sequence data. Bioinformatics 28: 1647–1649.

Mantilla-Meluk, H., A.M. Jimenez-Ortega, and R.J. Baker. 2009. Mammalia, Chiroptera, Phyllostomidae, *Lonchophylla pattoni*: first record for Ecuador. Investigación, Biodiversidad y Desarrollo 28: 222–225.

Mantilla-Meluk, H., H.E. Ramírez-Chaves, J.A. Parlos, and R.J. Baker. 2010. Geographic range extensions and taxonomic notes on bats of the genus *Lonchophylla* (Phyllostomidae) from Colombia. Mastozoología Neotropical 17: 295–303.

Moratelli, R., and D. Dias. 2015. A new species of nectar-feeding bat, genus *Lonchophylla*, from the Caatinga of Brazil (Chiroptera, Phyllostomidae). ZooKeys 514: 73–91.

Nogueira, M.R., R. Gregorin, and A.L. Peracchi. 2014. Emended diagnosis of *Xeronycteris vieirai* (Mammalia: Chiroptera), with the first record of polyodontia for the genus. Zoologia (Curitiba) 31: 175–180.

Paradis, E. 2012. Analysis of phylogenetics and evolution with R, 2nd ed. New York: Springer.

Parlos, J.A., R.M. Timm, V.J. Swier, H. Zeballos, and R.J. Baker. 2014. Evaluation of the paraphyletic assemblages within Lonchophyllinae, with description of a new tribe and genus. Occasional Papers, Museum of Texas Tech University 320: 1–23.

Phillips, C.J. 1971. The dentition of glossophagine bats: development, morphological characteristics, variation, pathology, and evolution. University of Kansas Museum of Natural History Miscellaneous Publications 64: 1–138.

Posada, D. 2008. jModelTest: Phylogenetic model averaging. Molecular Biology and Evolution, 25: 1253–1256.

Rambaut, A., and A.J. Drummond. 2007. Tracer, 1.6 ed. Online resource (http://tree.bio.ed.ac.uk/software/tracer/).

Ronquist, F., et al. 2012. MrBayes 3.2: efficient Bayesian phylogenetic inference and model choice across a large model space. Systematic Biology 61: 539–542.

Voss, R.S., and D.W. Fleck. 2011. Mammalian diversity and Matses ethnomammalogy in Amazonian Peru. Part 1: Primates. Bulletin of the American Museum of Natural History 351: 1–81.

Voss, R.S., D.W. Fleck, R.E. Strauss, P.M. Velazco, and N.B. Simmons. 2016. Roosting ecology of Amazonian bats: evidence for guild structure in hyperdiverse mammalian communities. American Museum Novitates 3870: 1–43.

Wetterer, A.L., M.V. Rockman, and N.B. Simmons. 2000. Phylogeny of phyllostomid bats (Mammalia: Chiroptera): data from diverse morphological systems, sex chromosomes, and restriction sites. Bulletin of the American Museum of Natural History 248: 1–200.

Woodman, N. 2007. A new species of nectar-feeding bat, genus *Lonchophylla*, from western Colombia and western Ecuador (Mammalia: Chiroptera: Phyllostomidae). Proceedings of the Biological Society of Washington 120: 340–358.

Woodman, N., and R.M. Timm. 2006. Characters and phylogenetic relationships of nectar-feeding bats, with descriptions of new *Lonchophylla* from western South America (Mammalia: Chiroptera: Phyllostomidae: Lonchophyllini). Proceedings of the Biological Society of Washington 119: 437–476.

APPENDIX 1

Specimens Examined

The following list includes all specimens used in the morphological components of this study with data on their respective localities. See Material and Methods for abbreviations. Coordinates are provided in appendix 2. Specimens used in the morphometric analyses are marked with an asterisk.

Hsunycteris cadenai (*N* = 7). COLOMBIA––*Valle del Cauca*: Bajo Calima, ca. 45 km by air NNE of Buenaventura, along the Río Calima (USNM 338726*); across from the Village of Zabaletas, east bank Rio Zabaleta, 29 km SE Buenaventura (USNM 446481, 446482, 483359 [holotype], 483363*, 483364*, 483365).

Hsunycteris dashe (*N* = 3). PERU––*Loreto*: Alto Amazonas, Nuevo San Juan, Gálvez River (AMNH 273165*; MUSM 15206* [holotype], 15211).

Hsunycteris pattoni (*N* = 37). BOLIVIA––*Beni*: 1.5 km below Costa Marquez, Itenez River (AMNH 209358*). *Santa Cruz*: Parque Nacional Kempff Mercado, Meseta de Huanchaca, Huanchaca I (USNM 584474, 584475*). BRAZIL––*Amazonas*: 80 km N by road of Manaus (USNM 530960, 530961, 530962*). *Para*: Altamira, 52 km SSW, E Bank Rio Xingu (USNM 549362*, 549363*, 549364). PERU––*Loreto*: Alto Amazonas, Nuevo San Juan, Gálvez River (AMNH 273069, 273093, 273124–273126; MUSM 13205*, 15207–15210); Maynas, Punchana, Barrio Orosa Estación Madreselva II, Río Amazonas (MUSM 31927–31930); Quebrada Blanco, Comunidad de Limón (MUSM 21173*); Requena, Jenaro Herrera, Centro de Investigaciones Jenaro Herrera (AMNH 278465*, 278500*; CEBIOMAS 100*, 101; MUSM 863*, 5523, 5541, 5542, 5589*, 5932*, 5933, 5940). *Madre de Dios*: Tambopata, north bank of the Río Madre de Dios, 14 km E Puerto Maldonado, Reserva Cuzco Amazónico (MUSM 24350* [holotype]).

Hsunycteris thomasi (*N* = 55). BRAZIL––*Amazonas*: 80 km N by road of Manaus (USNM 530959); Manaus, University (USNM 530958). *Para*: Altamira, 52 km SSW, E Bank Rio Xingu (USNM 549366*, 549367*, 549369); Belem, Fazenda Velha (USNM 361570, 361571); Belem, Mocambo (Igapo) (USNM 393013, 393014*); Belem, Utinga (USNM 460098); Belem, Varzea (USNM 460097*). ECUADOR––*Napo*: Río Yasuni (USNM 528325*). *Pastaza*: Tiguino, 130 km S of Coca (USNM 574510, 574511*). FRENCH GUIANA––*Cayenne*: Paracou, near Sinnamary (AMNH 266106, 266110, 267451, 267451, 267940, 267943). GUYANA––*Barima-Waini*: Baramita (USNM 582299, 582300*, 582301*). PANAMA––*Bocas del Toro*: Nuri (USNM 575486*, 575488*, 575489–575491, 575493, 575494, 575496, 575497*, 575498). *Darien*: mouth of Río Paya (USNM 306582). *San Blas*: Armila, Quebrada Venado (USNM 335180*). PERU––*Loreto*: Maynas, Río Maniti, Santa Cecilia (FMNH 87070*); Quebrada Blanco, Comunidad de Limón (MUSM 21170, 21171, 21172*); Requena, Jenaro Herrera, Centro de Investigaciones Jenaro Herrera (MUSM 5509, 5931). VENEZUELA––*Amazonas*: Capibara, 106 km SW Esmeralda, Brazo Casiquiare (USNM

415387); Casiquare Canal, Capibara (USNM 415388); Cerro Neblina Base Camp, Rio Mawarinuma (USNM 559186); Puerto Ayacucho, 32 km S Puerto Ayacucho, Raya (USNM 407802*, 407803); San Carlos de Río Negro, ca 7 km E (USNM 560560); San Juan, 163 km ESE Puerto Ayacucho, Río Manapiare (USNM 407798*, 407799*, 407801); Tamatama, Río Orinoco (USNM 407796, 407797*). *Bolívar*: Ciudad Bolívar (AMNH 16120 [holotype]); El Manaco, 59 km SE El Dorado, km 74 (USNM 385753); Icabaru, 45 km NE Icabaru, Santa Lucia de Surukun (USNM 456537).

APPENDIX 2

Gazetteer of Collecting Localities

Below we list the localities of all the specimens and/or tissues used in this study. Names of the largest administrative unit (department, state, etc.) within each country are italicized, and geographic coordinates are provided.

BOLIVIA

1. *Beni*, 1.5 km below Costa Marques (-12.4833, -64.3000).
2. *Santa Cruz*, Parque Nacional Kempff Mercado, Meseta de Huanchaca, Huanchaca I (-13.9075, -60.8147).

BRAZIL

3. *Amazonas*, 80 km N by road of Manaus (-2.4000, -59.7167).
4. *Amazonas*, Manaus, University (-3.1333, -60.0166).
5. *Pará*, Altamira, 52 km SSW, E Bank Rio Xingu (-3.6500, -52.3700).
6. *Pará*, Belém, Fazenda Velha (-1.4500, -48.4833).
7. *Pará*, Belém, Mocambo (Igapo) (-1.4500, -48.4833).
8. *Pará*, Belém, Utinga (-1.4500, -48.4833).
9. *Pará*, Belém, Varzea (-1.4500, -48.4833).
10. *Paraiba*, Fazenda Espírito Santo, near Campina Grande, Municipio de Soledade (-7.0833, -36.3500).

COLOMBIA

11. *Valle del Cauca*, Bajo Calima, ca. 45 km by air NNE of Buenaventura, along the Río Calima (4.0167, -77.0000).
12. *Valle del Cauca*, across from the Village of Zabaletas, east bank Rio Zabaleta, 29 km SE Buenaventura (3.7333, -76.9500).

ECUADOR

13 *Esmeraldas*, 2 km S Alto Tambo (0.9216, -78.5500).
14. *Esmeraldas*, Comuna San Francisco de Bogotá (1.0935, -78.7059).
15. *Esmeraldas*, Terrenos Aledaños de la Comuna San Francisco de Bogotá (ca. 1.0935, -78.7059).

16. *Esmeraldas*, E San Lorenzo, banana plantation (1.2586, -78.7808).
17. *Esmeraldas*, E San Lorenzo, La Guarapera farm and pasture (1.2702, -78.8030).
18. *Esmeraldas*, San Jose Farm, E San Lorenzo towards Lita (1.0100, -78.6222).
19. *Morona Santiago*, Huamboya, Cueva de los Tayos, por el río Paztaza (-1.936432, -77.793260).
20. *Napo*, Río Yasuni (-0.9300, -75.9500).
21. *Pastaza*, 5 km E Puyo, Safari Hosteria Park (-1.7333, -78.0000).
22. *Pastaza*, Puyo, Finca el Pigual (-1.4797, -77.9966).
23. *Pastaza*, Tiguino, 130 km S of Coca (-1.1167, -76.9500).
24. *Pichincha*, Mejía, La Unión del Toachi, Otongachi (-0.313829, -78.9544).

FRENCH GUIANA
25. *Cayenne*, Paracou, near Sinnamary (5.2833, -52.9167).

GUYANA
26. *Barima-Waini*, Baramita (7.3714, -60.4958).
27. *Potaro-Siparuni*, Iwokrama Reserve, 5 km SW of Kurupukari, Giadonda Camp (4.6333, -58.7167).

PANAMA
28. *Bocas del Toro*, Nuri (8.9167, -81.8167).
29. *Darién*, Cana (7.7833, -77.7000).
30. *Darién*, mouth of Río Paya (7.9167, -77.5167).
31. *San Blas*, Armila, Quebrada Venado (8.6667, -77.4500).

PERU
32. *Arequipa*, 2 km NE of Atiquipa, "El Castillo," (-15.7811, -74.3476).
33. *Huánuco*, 6 km N Tingo María (-9.2336, -75.9833).
34. *Lambayeque*, Las Juntas, in Quebrada La Pachinga, ca. 14 km N, 25 km E Olmos (-6.4500, -79.8667).
35. *Loreto*, Alto Amazonas, Nuevo San Juan, Gálvez River (-5.2500, -73.1667).
36. *Loreto*, Maynas, Punchana, Barrio Orosa Estación Madreselva II, Río Amazonas (-3.6277, -72.2401).
37. *Loreto*, Maynas, Río Manití, Santa Cecilia (-3.5555, -72.8833).
38. *Loreto*, Quebrada Blanco, Comunidad de Limón (ca. -4.3166, -73.2333).
39. *Loreto*, Requena, Jenaro Herrera, Centro de Investigaciones Jenaro Herrera (-4.8986, -73.6503).
40. *Loreto*, San Jacinto (-2.31667, -74.86667).
41. *4Madre de Dios*, Hacienda Erika, Río Alto Madre de Dios opposite Salvación (-12.8491, -71.3876).
42. *Madre de Dios*, Tambopata, north bank of the Río Madre de Dios, 14 km E Puerto Maldonado, Reserva Cuzco Amazónico (-12.5500, -69.0500).

SURINAM

43. *Brokopondo*, Brownsberg Nature Park, 8 km S, 2 km W of Brownsweg (4.9167, -55.1667).
44. *Brokopondo*, Marowijne, 3 km SW of Albina (5.4667, -54.0833).
45. *Nickerie*, Bitagron (Kayserberg Airstrip) (3.1000, -56.4667).

VENEZUELA

46. *Amazonas*, Capibara, 106 km SW Esmeralda, Brazo Casiquiare (2.6200, -66.3200).
47. *Amazonas*, Casiquiare Canal, Capibara (2.6167, -66.3167).
48. *Amazonas*, Cerro Neblina Base Camp, Río Mawarinuma (0.8300, -66.1700).
49. *Amazonas*, Puerto Ayacucho, 32 km S Puerto Ayacucho, Raya (5.4000, -67.6500).
50. *Amazonas*, San Carlos de Río Negro, ca 7 km E (1.9167, -67.0667).
51. *Amazonas*, San Juan, 163 km ESE Puerto Ayacucho, Río Manapiare (5.3000, -66.2200).
52. *Amazonas*, Tamatama, Río Orinoco (3.1700, -65.8200).
53. *Bolívar*, Ciudad Bolívar (8.1333, -63.5500).
54. *Bolívar*, El Manaco, 59 km SE El Dorado, Km 74 (6.2800, -61.3200).
55. *Bolívar*, Icabarú, 45 km NE Icabarú, Santa Lucia de Surukun (4.5500, -61.4200).
56. *Bolívar*, Río Grande, 28 km E El Palmar (8.0067, -61.6972).

APPENDIX 3

Principal Component Factor Loadings

Loadings for the first three factors extracted from a principal components analysis of 12 measurement variables. See Material and Methods for definitions and abbreviations of variables.

Measurements	PC 1	PC 2	PC 3
FA	0.100	0.052	0.511
GLS	0.228	0.028	-0.158
CIL	0.259	0.138	-0.141
CCL	0.260	0.173	-0.101
BB	0.188	-0.117	0.161
C–C	0.302	-0.243	0.424
MPW	0.260	0.055	0.241
MTRL	0.263	0.480	-0.183
M2–M2	0.190	0.219	0.534
DENL	0.268	0.209	-0.125
MANDL	0.252	0.463	-0.090
COH	0.608	-0.579	-0.280
Proportion of variance (%)	56.3	14.9	11.1

APPENDIX 4

Matrix of Genetic Distances

Average percent uncorrected (p) and Kimura 2-parameter (K2P) genetic distances for *Hsunycteris* species estimated using the R package ape v4.1. All sequences were cropped to the first 400 bp of the mitochondrial *Cyt-b* gene. Uncorrected-p distances shown below the diagonal and K2P distances shown above the diagonal. Values along the diagonal represent within group K2P pairwise distances for each *Hsunycteris* group.

	1	2	3	4	5
1. *H. cadenai*	**0.5**	14.0	13.4	13.4	11.4
2. *H. dashe*	12.4	–	12.2	15.0	12.8
3. *H. pattoni*	11.9	10.9	**1.8**	7.9	8.5
4. *H. thomasi* A	13.2	13.2	7.4	**0.3**	8.1
5. *H. thomasi* B	11.4	11.4	5.2	7.6	**2.3**

All issues of *Novitates* and *Bulletin* are available on the web (http://digitallibrary.amnh.org/dspace). Order printed copies on the web from:
http://shop.amnh.org/a701/shop-by-category/books/scientific-publications.html

or via standard mail from:

American Museum of Natural History—Scientific Publications
Central Park West at 79th Street
New York, NY 10024

♾ This paper meets the requirements of ANSI/NISO Z39.48-1992 (permanence of paper).